Allergy Asthma Immunol Res. 2023 Mar;15(2):246-261
https://doi.org/10.4168/aair.2023.15.2.246
pISSN 2092-7355·eISSN 2092-7363

Allergy, Asthma & Immunology Research AAIR

Original Article

Allergic Sensitization Driving Immune Phenotyping and Disease Severity in a Mouse Model of Asthma

Eléonore Dijoux,[1] **Martin Klein**,[1] **Barbara Misme-Aucouturier**,[2] **Marie-Aude Cheminant**,[1] **Marion de Carvalho**,[2] **Louise Collin**,[1] **Dorian Hassoun**,[1] **Erwan Delage**,[3] **Mathilde Gourdel**,[1,4] **Gervaise Loirand**,[1] **Vincent Sauzeau**,[1] **Antoine Magnan**,[5,6] **Grégory Bouchaud**[1,2*]

[1]Nantes Université, CNRS, INSERM, L'institut du Thorax, Nantes, France
[2]INRAe, Biopolymères Interactions Assemblages (BIA), Nantes, France
[3]Université de Nantes, CNRS UMR 6004, LS2N, Nantes, France
[4]CRNH-Ouest Mass Spectrometry Core Facility, Nantes, France
[5]Hôpital Foch, Suresnes, France
[6]UMR 0892 Virologie et Immunologie Moléculaire, Université de Versailles Saint-Quentin-en-Yvelines (UVSQ), Université Paris-Saclay INRAE, Paris, France

Received: Jun 30, 2022
Revised: Sep 30, 2022
Accepted: Oct 17, 2022
Published online: Jan 3, 2023

Correspondence to
Grégory Bouchaud, PhD
INRAe, Biopolymères Interactions Assemblages (BIA), Rue de la Géraudière, 44000 Nantes, France.
Email: gregory.bouchaud@inrae.fr

ORCID iDs
Eléonore Dijoux
https://orcid.org/0000-0001-9228-0203
Martin Klein
https://orcid.org/0000-0003-3274-2415

ABSTRACT

Purpose: Asthma is a frequent chronic inflammatory bronchial disease affecting more than 300 million patients worldwide, 70% of whom are secondary to allergy. The diversity of asthmatic endotypes contributes to their complexity. The inter-relationship between allergen and other exposure and the airway microbiome adds to the phenotypic diversity and defines the natural course of asthma. Here, we compared the mouse models of house dust mite (HDM)-induced allergic asthma. Allergic sensitization was performed via various routes and associated with outcomes.
Methods: Mice were sensitized with HDM via the oral, nasal or percutaneous routes. Lung function, barrier integrity, immune response and microbiota composition were analyzed.
Results: Severe impairment of respiratory function was observed in the mice sensitized by the nasal and cutaneous paths. It was associated with epithelial dysfunction characterized by an increased permeability secondary to junction protein disruption. Such sensitization paths induced a mixed eosinophilic and neutrophilic inflammatory response with high interleukin (IL)-17 airway secretion. In contrast, orally sensitized mice showed a mild impairment of respiratory function. Epithelial dysfunction was mild with increased mucus production, but preserved epithelial junctions. Regarding lung microbiota, sensitization provoked a significant loss of diversity. At the genus level, *Cutibacterium*, *Acinetobacter*, *Streptococcus* and *Lactobacillus* were found to be modulated according to the sensitization pathway. An increase in theanti-inflammatory microbiota metabolites was observed in the oral-sensitization group.
Conclusions: Our study highlights the strong impact of the sensitization route on the pathophysiology and the critical phenotypic diversity of allergic asthma in a mouse model.

Keywords: Respiratory function; barrier integrity; endotypes; lung microbiota

Barbara Misme-Aucouturier
https://orcid.org/0000-0002-6148-151X
Dorian Hassoun
https://orcid.org/0000-0002-2154-0474
Erwan Delage
https://orcid.org/0000-0002-7653-5111
Gervaise Loirand
https://orcid.org/0000-0002-2306-3931
Vincent Sauzeau
https://orcid.org/0000-0002-6187-0312
Antoine Magnan
https://orcid.org/0000-0002-9282-6656
Grégory Bouchaud
https://orcid.org/0000-0002-3794-7287

Disclosure
There are no financial or other issues that might lead to conflict of interest.

INTRODUCTION

Asthma is an inflammatory disease of the airways which leads to recurrent episodes of cough, dyspnea, wheezing and chest tightness.[1] The pathogenesis of allergic asthma, which accounts for up to 70% of cases, involves exposure to allergens and mediation by immunoglobulin E (IgE).[2-4] However, the immunopathological mechanism, initially mediated by IgE, is much more complex, and includes inflammatory mediators and cytokines, with a predominance of T helper 2 lymphocytes (Th2 cells).[5] Given that the development of asthma is not confined to young children and occurs at all ages, it is important to determine whether and how exposure history affects the sensitizing responses to allergens. Heterogeneity in clinical presentations of asthma prevents the development of a pertinent experimental animal model.[6,7] Indeed, animal models of asthma are typically based on artificial routes of sensitization (*e.g.*, intraperitoneal injection) and well-studied synthetic adjuvants (*e.g.*, alum) that induce Th2-dominant, eosinophilic airway inflammation after allergen re-exposure.[8,9] More recent approaches through airway exposure have shown that allergic sensitization occurs when allergens are administered with an adjuvant such as LPS, whereas administration of a protein alone causes a suppressive and tolerogenic response to allergens.[10-13] In naive hosts, subtle differences in the dose and timing of adjuvant exposure can translate into significant differences in the quantity and quality of mucosal effector responses induced following allergen re-exposure typically involving Th2- or Th2/Th17-dependent airway inflammation.[14] In contrast, the tolerogenic response involves IL-10-producing dendritic cells, regulatory T cells (Tregs) and limited inflammation.[15-19] However, most studies to date have focused on the events following mucosal sensitization in naive hosts, and very little is known about how tolerance shapes the development of subsequent immunity. Furthermore, the microbiota has been identified as a key factor in many chronic inflammatory diseases including asthma. In fact, the lung microbiota shows different compositions of bacterial populations, which are correlated with the degree of asthma severity.[20] This interaction is based on bacterial metabolite communication through short free fatty acids, such as butyrate. Most asthma models with mice use ovalbumin as a foreign sensitizing protein associated with an adjuvant. Nevertheless, we and others have developed house dust mite (HDM) models of allergic asthma without adjuvants to mimic sensitization in a closer manner to the clinical features of human asthma.[21] Therefore, models with oral, cutaneous or respiratory sensitization, which are more clinically relevant routes involved in the pathogenesis of human allergic asthma, have been used.[22,23] Our group demonstrated that cutaneous sensitization induces a mixed Th2/Th17 allergic asthma endotype associated with mixed neutrophilic and eosinophilic airway inflammation.[21] Nevertheless, there have been few studies about the influence of sensitization route on the asthma phenotype associated with an impact on the immune response, lung barrier function and microbiota dysbiosis. Here, we compared mouse models of HDM-induced allergic asthma via different routes in regard to clinical features of asthma, immune responses, lung barrier and dysbiosis.

MATERIALS AND METHODS

Animal model

BALB/c By J female mice were obtained from Charles River (Lyon, France). These mice were housed in ventilated cages in the IRS-1 Experimental Therapeutics Unit with free access to water and a standard diet (SAFE A04) with a dark/light cycle of 12:12 hours. The total extract of HDMs was obtained from Stallergen Greer (Antony, France).

https://doi.org/10.4168/aair.2023.15.2.246

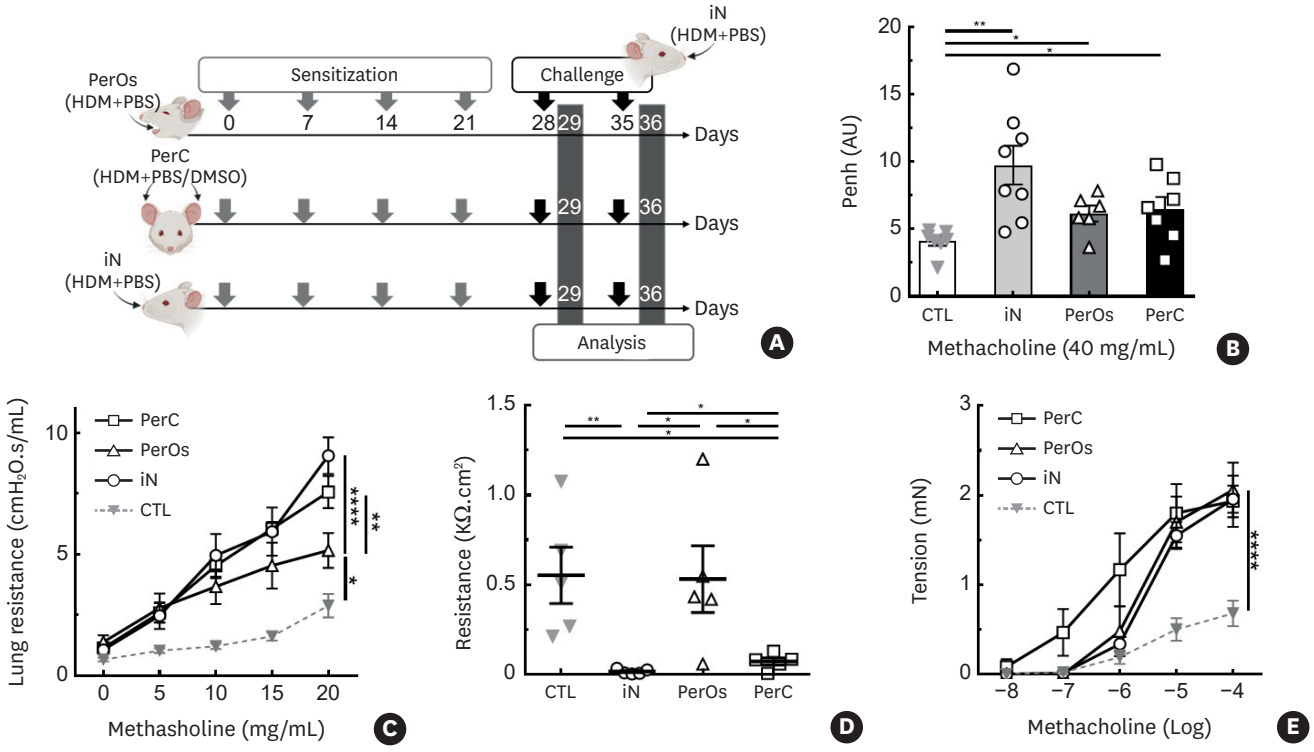

Fig. 1. The sensitization route has an impact on respiratory function with different degrees of severity. (A) Mice were sensitized to HDMs either iN, PerOs, or PerC to trigger the allergic reaction, and the CTL received PBS. (B) The expiratory pause time (Penh) was analyzed by plethysmography. (C) Airway resistance was measured by the forced oscillation technique (n = 7). (D) Tracheal resistance was determined in an Ussing chamber. (E) Bronchial smooth muscle contractility was evaluated using Mulvany's isometric myograph. The white bar or the gray triangle indicates the CTL mice, the light gray bar or the white circle indicates the iN, the dark gray bar or the white triangle indicates the PerOs, and the black bar or the white square indicates the PerC. Data are represented as the mean ± standard error of mean (n = 5–7).
HDM, house dust mite; iN, nasal route; PerOS, oral route; PerC, percutaneous route; CTL, control; PBS, phosphate-buffered saline; Penh, enhanced pause.
*P < 0.05, **P < 0.01, ****P < 0.001.

BALB/c By J female mice, aged 7 weeks, were sensitized once a week for four weeks with HDM diluted in phosphate-buffered saline (PBS) as described (**Fig. 1A**). Based on our previous work and on the literatures, we used different doses of HDM to sensitize animals according to different sensitization routes in order to reach comparable amount of allergen to pass through the epithelial barrier[24-26]: oral (20 mg of HDMs diluted in 200 µL of PBS), nasal (250 µg of HDMs diluted with 40 µL of PBS) or percutaneous (500 µg of HDMs diluted with 20 µL of DMSO 70%). After the sensitization phase, the mice were challenged twice intranasally (250 µg of HDM diluted with 40 µL of PBS), regardless of the initial route of sensitization to induce potent allergic reactions as previously described.[26] The control (CTL) mice received PBS alone. The final analysis was performed 24 hours after the last challenge.

Airway hyperresponsiveness (AHR) measurement

After the first challenge, the enhanced pause (Penh) variable was measured by whole body plethysmography (emka TECHNOLOGIES, Paris, France). A conscious mouse was kept alone in a plethysmography chamber, and the airways flow and pressure were measured before and after nebulization of increasing concentration of methacholine (Mch) from 0 to 40 mg/mL. To confirm AHR, airway resistance was evaluated using the force oscillation technique (emka TECHNOLOGIES). After mice were anesthetized and intubated, airway resistance and compliance were measured before and after nebulization of increasing concentrations of Mch from 0 to 20 mg/mL.

https://doi.org/10.4168/aair.2023.15.2.246

Tracheal resistance

Tracheas were extracted from the mice and fit in Ussing chambers (Physiologic Instruments, San Diego, CA, USA). The spontaneous transepithelial potential difference (PD) was measured, and the tissue was adjusted at zero voltage by continuously introducing an appropriate short-circuit current with an automatic voltage clamp (Physiologic Instruments). Tissue ion resistance (1/G), where G is conductance, was measured from the potential difference and short-circuit current according to Ohm's law using the Acquire and Analyze software (Physiologic Instruments).

Bronchial contraction

Bronchi were extracted from the lung and fit in a Mulvany myograph chamber (Scintica, London, England). Bronchial contraction viability was determined first through an acetylcholine challenge. The maximal temporary bronchial contraction was evaluated with a Mch challenge.

Histology

Lungs were fixed in 4% paraformaldehyde in PBS for at least 48 hours, embedded in paraffin, cut and stained by MicropiCell Platform (SFR Bonamy, IRS-UN, Nantes, France). Periodic acid-Schiff (PAS) and hematoxylin-phloxine-saffron (HPS) staining were used to assess mucus production and inflammatory infiltrate/epithelial integrity, respectively. Bronchial smooth muscle hyperplasia was analyzed by transgelin staining (anti-TAGLN/transgelin antibody [ab14106]; Abcam, Cambridge, UK). Large lung scans were performed with a Nikon Eclipse Ti2 microscope (NIS-Element). The histological score was based on the following criteria: integrity and hyperplasia of the lung epithelium (measure of the increase in epithelial thickness), lung inflammatory infiltrate (observation of inflammatory infiltrate or nodules), presence of mucus cells and mucus production, and bronchial smooth muscle remodeling (measure of the increase in smooth muscle thickness). Each of the 4 criteria was graded on a 5-point scale with a relative comparison to CTL mice, for a final score of 20 points.

Bronchoalveolar lavage (BAL)

BAL was obtained by filling airways with 5×1 mL of PBS buffer. BAL was centrifuged to pellet cells that were counted and analyzed by flow cytometry. The pellet was suspended in prelysis buffer and proteinase K, and immediately frozen at −80 °C for microbiota DNA extraction. The supernatant was kept for microbiota metabolite and cytokine analyses. BAL cytokine quantification was processed with Bio-plex Pro™ Mouse Cytokine Grp1 Panel 23-Plex (Bio-Rad Laboratories, Hercules, CA, USA) according to the manufacturer's instructions using the Bioplex® 200 system of Bio-Rad.

Analysis of microbiota composition

Bacterial DNA was extracted from BAL pellets according to the manufacturer's instructions (genomic DNA from tissue, NucleoSpin™ Tissue; Macherey-Nagel, Düren, Germany). The microbiota composition was analyzed by 16S sequencing with permission from Biofortis (Saint-Herblain, France). Raw sequencing data were obtained from a single Illumina MiSeq run as 250 bp paired-end reads targeting the V3-V4 region (Primers: Bakt_341F 5′-CCTACGGGNGGCWGCAG-3′, Bakt_805R 5′-GACTACHVGGGTATCTAATCC-3) of the 16S rDNA gene. Reads were processed with microSysMics (https://bio.tools/microSysMics), a workflow built around the QIIME2 toolbox, chaining softwares in order to automatize metabarcoding analysis. PCR primers and remaining Illumina adapters were removed with Cutadapt. Amplicon sequence variants (ASVs) inference and count estimation were

https://doi.org/10.4168/aair.2023.15.2.246

performed with dada2 using a trimming length of 220 and default parameters. We used a Naive Bayes Classifier pre-trained on the SILVA 99% reference database (release 138) to assign ASVs to taxa.

Analysis of microbiota metabolites

First, in silico analysis of microbiota metabolite production was performed based on 16S sequencing results. Based on these results, all of the different families of metabolites identified were investigated by mass spectrometry.

Flow cytometry

Lungs were removed and crushed with a Tenbroeck tissue grinder (Wheaton™; DWK Life Sciences, Mainz, Germany) to obtain a single-cell suspension. The lung pellet was suspended in 1 mL of RBC Lysis Buffer (eBioscience™; Thermo Fisher Scientific, Waltham, MA, USA) to lyse erythrocytes for 8 minutes at room temperature, mixed with 9 mL of fluorescence-activated cell sorting (FACS) buffer (Dulbecco's Phosphate Buffered Saline without Ca^{2+} and Mg^{2+}, 1% ethylenediaminetetraacetic acid, 1% fetal bovine serum). The lung cell pellet was suspended in 600 µL of FACS buffer. Total cells were counted on KOVA slides. BAL cells were stained with the following surface markers: CD3-PerCP Cy5.5, CD4-APC Cy7, CCR3-Alexa647, F4/80-FITC, Ly6G-BV421, Siglec F-BV510 and Ly6C-PE. T-cell lymphocytes in the lung were stained with the following surface markers: CD3-PerCP Cy5.5, CD4-APC Cy7, CD8-FITC and CD25-BV510. The cells were fixed and permeabilized using the Cytofix/Cytoperm Kit (BD Biosciences, Franklin Lakes, NJ, USA) and stained with Fox P3-Alexa647, GATA3-PE-Cy7 and RORγT-PE. The cells were identified by flow cytometry on a Fortessa X20 cytometer (BD Biosciences). Data were acquired using DIVA software (BD Biosciences) and analyzed with FlowJo (TreeStar, V10.5.3).

Real-time quantitative polymerase chain reaction (RT-qPCR)

Lungs were dissociated in lysis buffer using a TissueLyser II (Qiagen, Hilden, Germany) 2 times for 3 minutes at 30 Hz with one bead mill. Total RNA was extracted with the NucleoSpin RNA/Protein Mini kit for RNA and protein purification (Macherey-Nagel). RNA quality was determined by measuring the 260/230 and 260/280 ratios with a Nanodrop system (Thermo Fisher Scientific). Twenty micrograms of total mRNA were reverse transcribed into cDNA with the High-Capacity cDNA Reverse Transcription kit of Applied Biosystems (Waltham, MA, USA) on a GeneAmp PCR system 9700. cDNA was stored at −20°C until use. RT-qPCR was performed in 384-well plates in triplicate with TaqMan™ Universal PCR Master Mix (Thermo Fisher Scientific). RT-qPCR was performed on a 7900HT Fast Real Time PCR System thermocycler. The following genes were assessed: zonula occludens-1 (ZO-1, Mm01320638_m1; Thermo Fisher Scientific), occludin (Mm00500912_m1; Thermo Fisher Scientific), E-cadherin (Mm01247357_m1; Thermo Fisher Scientific), vimentin (Vim, Mm01333430_m1; Thermo Fisher Scientific), mucin 2 (Muc2, Mm00458310_g1; Thermo Fisher Scientific) and mucin 5AC (Muc5ac, Mm01276731_g1; Thermo Fisher Scientific). Glyceraldehyde 3-phosphate dehydrogenase (Mm99999915_g1; Thermo Fisher Scientific) was used as a housekeeping control. The results were analyzed with the $2^{-\Delta\Delta Ct}$ method with CTL mice as the calibrator.

Enzyme-linked immunosorbent assay (ELISA)

Blood was collected by cardiac puncture and serum was collected. Specific Derf1 IgE was quantified in serum by indirect ELISAs. Ninety-six-well plates were coated with 2.5 µg/mL natural Derf1 (NA-DF11; Indoor Biotechnologies Ltd., Cardiff, UK) and left overnight at 4°C. Then, the wells were washed with PBS-0.1% Tween and saturated with PBS-0.1% Tween-0.5% gelatin (PBS-T-G) for 2 hours at 37°C, washed, filled with serum diluted by 40x in PBS-T-G and

https://doi.org/10.4168/aair.2023.15.2.246

incubated overnight at 4°C. Specific Derf1 IgE was revealed with anti-mouse IgE (CliniSciences, Nanterre, France) coupled to AP. Substrate MUPs (Merck, Sigma-Aldrich, St. Louis, MO, USA) were added for 1 hour 30 minutes at room temperature in the dark, and fluorescence was measured at 360 nm excitation and 440 nm emission with a Varioskan LUX 3020-956 (Thermo Fisher Scientific). Relative fluorescence was determined compared to that of the CTL mice.

Statistical analysis

Data were analyzed using GraphPad Prism 6.0 (La Jolla, CA, USA). Values are expressed as the mean ± standard error of mean, and were compared using nonparametric analysis of variance with a Kruskal-Wallis test. A *P* value of less than 0.05 was considered significant.

Ethics approval and consent to participate

All experiments followed ethical rules, and the protocol was approved by the ethics committee on Animals Experimentation Pays de Loire (accreditation number 17265).

RESULTS

The oral route is less effective in inducing allergic lung dysfunction in asthma than the other routes

To evaluate the impact of the sensitization route on the development of allergic asthma features in mice, we used models generated by HDM sensitization via the oral (PerOS), nasal (iN) or cutaneous (PerC) route (**Fig. 1A**). We first measured the impact on respiratory function in response to Mch (**Fig. 1B**). Following exposure to high dose of Mch, an increase in the Penh was observed in the sensitized mice compared to the CTL mice, regardless of the sensitization route. Then, we measured the lung resistance of the small airways and demonstrated an increase in lung resistance in the sensitized mice (**Fig. 1C**). Interestingly, the mice sensitized via the nasal or cutaneous route displayed a more increase in lung resistance compared to the orally sensitized mice, suggesting more severe lung dysfunction. To determine whether the sensitization route could also affect epithelial physiology, we measured tracheal electrical resistance in an Ussing chamber (**Fig. 1D**). We showed that tracheal resistance was increased in the iN and PerC groups compared to the CTL mice. However, the PerOS group displayed tracheal resistance similar to that of the CTL group. Airway smooth muscle (ASM) responses were characterized *in vitro* in isolated trachea (**Fig. 1E**). In accordance with airways resistance, ASM contraction in response to Mch was increased in the sensitized mice compared to the CTL mice. Taken together, our results indicated modulation of respiratory dysfunction toward a more severe phenotype in the percutaneously or nasally sensitized mice compared to the orally sensitized mice.

The sensitization route differentially affects the anatomic lung structure and epithelium integrity

To determine the impact of the sensitization route on macroscopic asthma features and bronchial epithelium integrity, we performed histological staining of the bronchi (**Fig. 2A**). Our results showed an increase in the histological score in the sensitized mice compared to the CTL mice, regardless of the sensitization route in terms of epithelial thickness, inflammatory infiltration, mucus production and smooth muscle thickness (**Supplementary Fig. S1A-D**). Epithelial barrier integrity was evaluated by the lung expression of the tight junction proteins, ZO-1, vimentin (Vim), E-cadherin (E-cad) and mucin 5AC (MUC5AC) (**Fig. 2B**). Surprisingly, ZO-1 expression was found to be similar in the iN, PerOS and CTL groups, but significantly

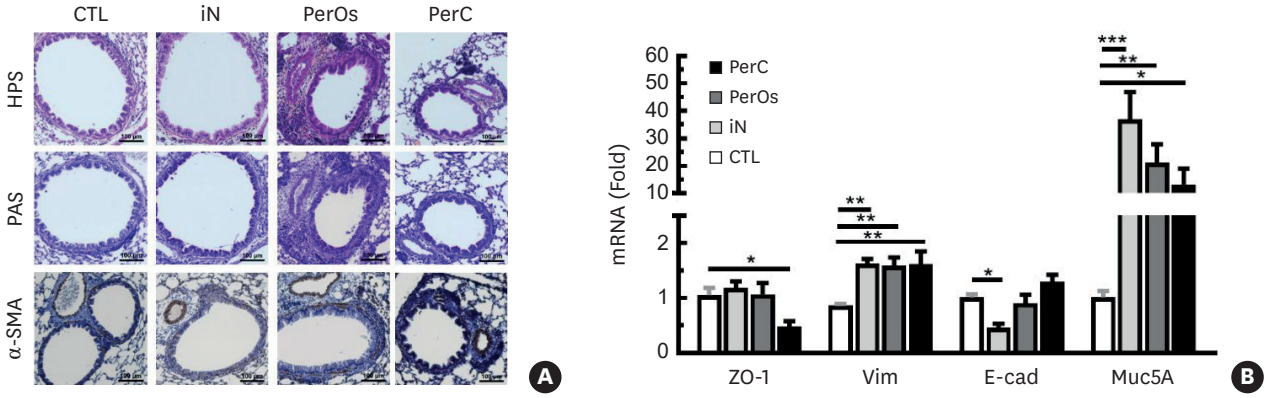

Fig. 2. The sensitization route modifies the anatomical and lung structural lesions. Lung sections were stained with HPS, PAS or transgelin staining (α-smooth muscle actin; α-SMA) after paraffin inclusion and observed under a microscope. (A) Airway epithelium thickness and inflammatory infiltrate were measured with HPS staining, and airway smooth muscle thickness was measured with α-SMA staining. (B) Relative mRNA expression of the tight junction proteins ZO-1, Vim, E-cad, and occludin was quantified by RT-qPCR. The white bar shows the CTL mice, the light gray bar shows the iN, the dark gray bar shows the PerOs and the black bar shows the PerC. Data are represented by the mean ± standard error of mean (n = 4–6).
HPS, hematoxylin-phloxine-saffron; PAS, periodic acid-Schiff; SMA, smooth muscle actin; ZO-1, zonula occludens-1; Vim, vimentin; E-cad, E-cadherin; RT-qPCR, real-time quantitative polymerase chain reaction; iN, nasal route; PerOS, oral route; PerC, percutaneous route; CTL, control; Muc5A, mucin 5AC.
$^{*}P < 0.05$, $^{**}P < 0.01$, $^{***}P < 0.005$.

reduced in the PerC group compared to the other groups, suggesting a more damaged epithelium integrity. In contrast, we found an increase in Vimentin expression in the sensitized mice compared to the CTL mice, regardless of the route of exposure. Our results indicated that the epithelium may undergo epithelial-mesenchymal transition (EMT) in the sensitized mice. Consistent with these results, the expression of E-cadherin, a crucial type of cell–cell adhesion molecule, was decreased in the iN mice compared to the CTL and the other mice, indicating that epithelial integrity affects EMT more definitely in the nasally sensitized mice. As a part of the epithelial barrier, mucus-secreting cells might be affected by the sensitization route. Therefore, we measured the expression of MUC5AC and found its overexpression in sensitized mice which can contribute to asthma. Altogether, our results suggested that the route of sensitization may influence epithelial barrier damage in different ways.

The sensitization route modifies the inflammatory profile and T cell responses

To determine the potential impact of the sensitization route on the asthma endotype, we analyzed inflammatory cells in BAL (**Fig. 3**). As expected, our model is characterized by eosinophilia (**Fig. 3A**). Interestingly, we observed a mixed eosinophil/neutrophil infiltration. The iN and PerC mice demonstrated a two-fold increase in neutrophilia compared to the PerOS mice. Similarly, we observed an increase in macrophages and lymphocytes in the iN and PerC mice, but did not in the PerOS mice. Then, we assessed the levels of RANTES (CCL5) and eotaxin (CCL11) in BAL (**Fig. 3B and C**). We observed an increase in RANTES and eotaxin productions in the iN and PerC mice compared to the CTL and PerOS mice, likely correlating with the T cell infiltration (**Fig. 3B**). In addition, eotaxin production was significantly increased in the iN mice compared to the PerC mice, suggesting modulation of eosinophilia by the sensitization route (**Fig. 3C**). Finally, we explored the effect of the sensitization route on Th2 humoral response defined by circulating HDM-specific IgE (**Fig. 3D**). Overall, asthmatic mice had a higher level of HDM-specific IgE than the CTL mice. The iN and PerC mice displayed a higher level of HDM-specific IgE than the PerOS mice. As our model induced mixed infiltration, we quantified pulmonary Th2, Th17, Treg cells and associated cytokines (**Fig. 4**). A strong type 2 response in the lungs was observed in asthmatic mice, regardless of the sensitization route (**Fig. 4A**). Accordingly, the levels of IL-4, IL-5, and IL-13 were increased

https://doi.org/10.4168/aair.2023.15.2.246

in asthmatic mice (**Fig. 4B**). However, the iN mice displayed a higher level of IL-4 than the other sensitized mice, and the PerOS mice showed a higher level of IL-4 than the PerC mice. An increase in Th17 cells was observed in the lungs of the iN and PerC mice, but not the PerOS mice, compared to the CTL mice (**Fig. 4C**). Moreover, the increase in Th17 cells was more pronounced in the PerC mice than in the iN mice, highlighting the influence of the sensitization route on the immune response in allergic asthma. Accordingly, the level of IL-17 was increased in the iN and PerC asthmatic mice compared to the CTL and PerOs mice (**Fig. 4D**). Treg cells were increased in the iN and PerC mice compared to the CTL and PerOS mice (**Fig. 4E**). Unlike Treg cells, IL-10 production was increased in the PerOS mice compared to the CTL, iN and PerC mice, suggesting a more pronounced regulatory response in the PerOS mice (**Fig. 4F**). The transforming growth factor (TGF)-β levels were increased in the asthmatic mice compared to the CTL mice, regardless of the route of sensitization (**Fig. 4G**). These results suggested that the route of sensitization may influence not only the inflammatory Th2 and Th17 responses, but also the regulatory response with opposing effects of the nasal and cutaneous routes versus the oral route. Our results demonstrated that the sensitization route can considerably modify lung inflammation at the cellular and molecular levels, humoral responses toward HDM and T cell responses.

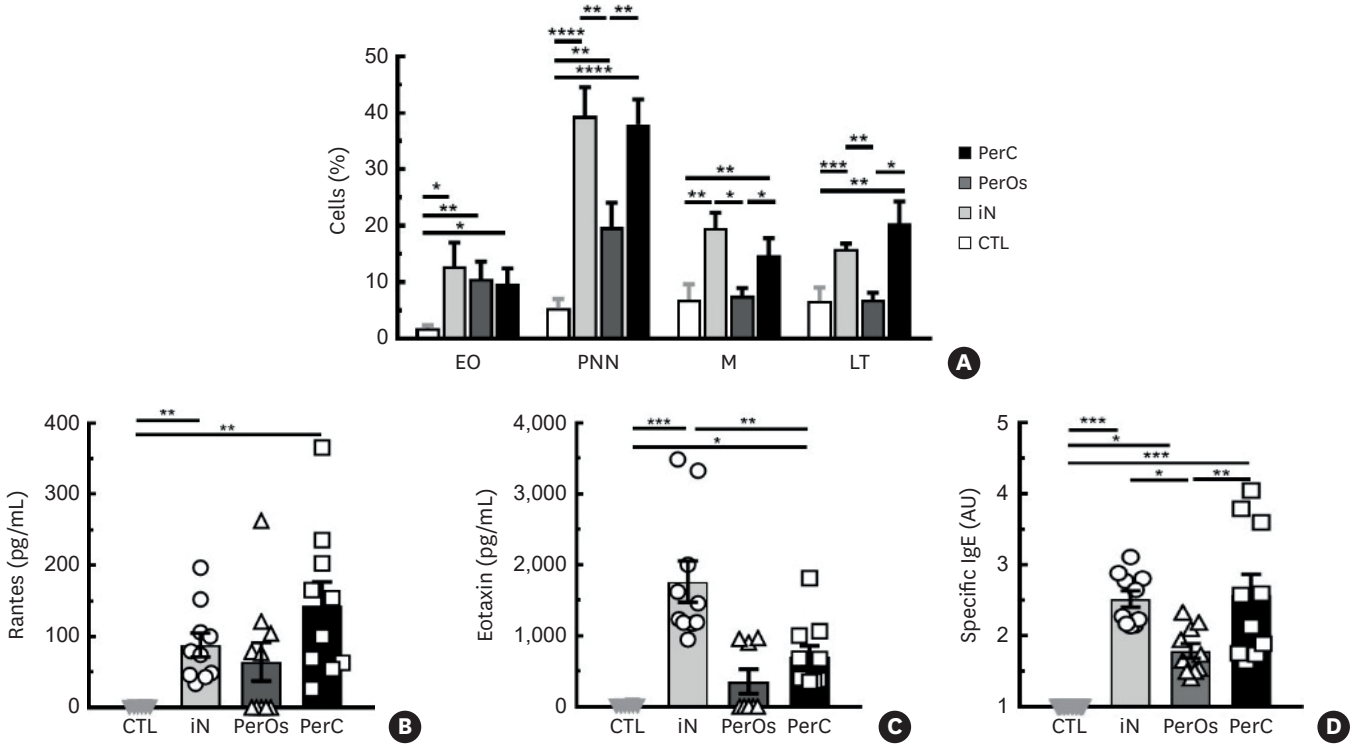

Fig. 3. The sensitization route influences inflammatory asthma markers. Lung inflammation was assessed by quantification by flow cytometry of EO, PNN, M and CD4+ LT present in BAL. (A) The results are expressed as the cell frequency (%). (B) Eotaxin and (C) Rantes cytokine levels were quantified by Bioplex technology. (D) Specific Derf1 IgE levels were quantified by ELISAs and are represented by their relative quantification to the CTL group (%). The white bar shows the CTL, the light gray bar shows the iN, the dark gray bar shows the PerOs, and the black bar shows the PerC. Data are represented as the mean ± standard error of mean (n = 4–6).
EO, eosinophils; PNN, neutrophils; M, macrophages; LT, T lymphocytes; BAL, bronchoalveolar lavage; ELISA, enzyme-linked immunosorbent assay; CTL, control; iN, nasal route; PerOS, oral route; PerC, percutaneous route.
*P < 0.05, **P < 0.01, ***P < 0.005, ****P < 0.001.

https://doi.org/10.4168/aair.2023.15.2.246

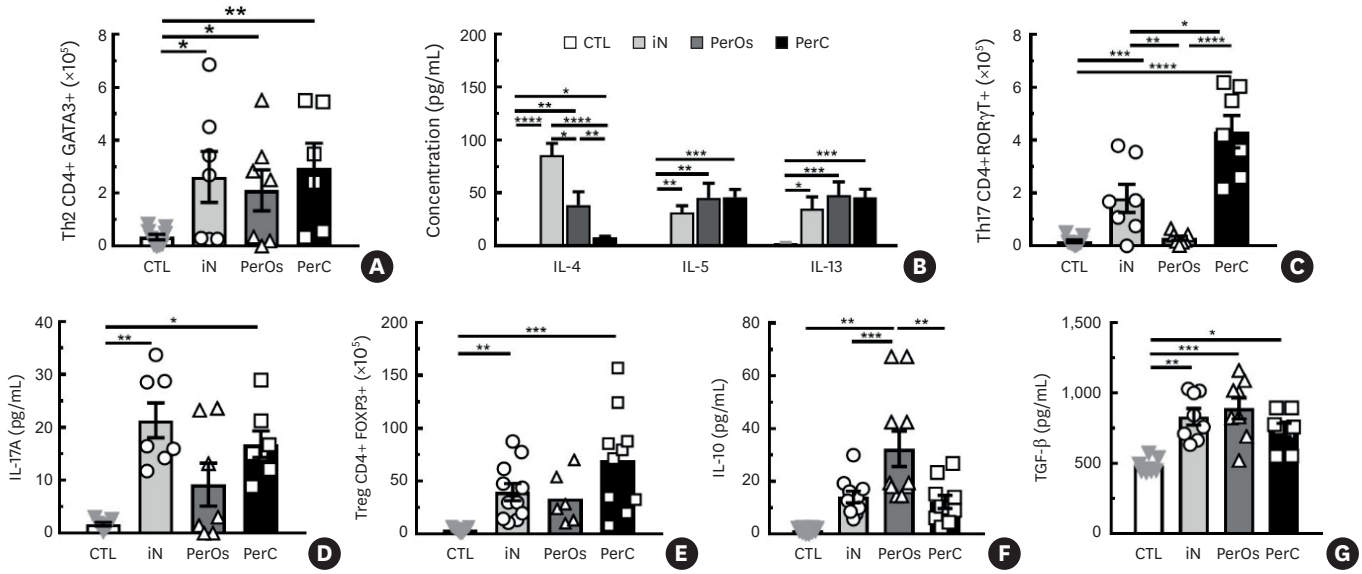

Fig. 4. The sensitization route has different impacts on the lung T-cell lymphocyte response. (A) Th2 lymphocytes and CD4+ GATA 3+ cells were quantified by flow cytometry in the lungs. (B) Cytokines secreted by Th2 lymphocytes, such as IL-4, IL-5 and IL-13, were quantified by BAL with Bioplex technology. (C) Th17 lymphocytes and CD4+ RORγT+ cells were quantified by flow cytometry in the lungs. (D) Cytokines secreted by Th17 lymphocytes, such as IL-17, were quantified by Bioplex technology. (E) Treg and CD4+ FOXP3+ cells in the lung were quantified by flow cytometry. (F) Cytokines secreted by Treg lymphocytes, such as TGF-β, were quantified in BAL by ELISAs and (G) IL-10 by Bioplex technology. The white bar shows the CTL, the light gray bar shows the iN, the dark gray bar shows the PerOs, and the black bar shows the PerC. Data are represented by the mean ± standard error of mean (n = 5–7).
Th, T helper; IL, interleukin; BAL, bronchoalveolar lavage; Treg, regulatory T cell; TGF, transforming growth factor; ELISA, enzyme-linked immunosorbent assay; CTL, control; iN, nasal route; PerOS, oral route; PerC, percutaneous route.
*P < 0.05, **P < 0.01, ***P < 0.005, ****P < 0.001.

The sensitization route is associated with different lung microbiota compositions

As asthma is a chronic inflammatory disease that shows complex heterogeneity with various phenotypes, depending on environmental factors and host characteristics, and the influence of the sensitization route on the inflammatory phenotype has been shown, we aimed to analyze the impact of the sensitization route on the lung microbiota (**Fig. 5**). Our results showed that the asthmatic mice had a lower bacterial diversity (**Fig. 5A**) and more ASVs (**Fig. 5B**) than the CTL mice. Then, the lung microbiota composition was measured, and we observed a decrease in *Cyanobacteria* and *Actinobacteriota,* and an increase in *Bacteroidota* abundance in the iN and PerC mice compared to the CTL mice. In contrast, the PerOS mice displayed a decrease in all these phyla. Additionally, the PerOS group had a specific increase in *Proteobacteria* abundance together with a decrease in *Firmicutes* abundance compared to other groups (**Fig. 5C**). Altogether, our results indicated specific changes in lung microbiota composition, depending on the route of sensitization. A significant decrease was observed in the abundances of four genera, *Cutibacterium, Acinetobacter, Lactobacillus* and *Streptococcus,* in the asthmatic mice compared to the CTL mice (**Fig. 5D-G**). However, no significant differences were observed in these genera, regardless of the route of sensitization, suggesting potential differences in bacterial activities. For the metabolites, we observed an increase in choline production, a component of cell membranes, and very low-density lipoproteins in the PerOS mice compared to the CTL mice (**Fig. 6A**). This result is in accordance with the modulation in *Proteobacteria* and *Firmicutes* abundance observed in the PerOS mice, as two phyla were involved in the metabolism of dietary choline. Similarly, two quaternary ammonium compounds, betaine and carnitine, which are involved in *Bacteroidetes* metabolism, were found to be increased in the PerOS mice compared to the other mice (**Fig. 6B**). Finally, another compound, taurine, implicated in feedback inhibition of the neutrophil/macrophage respiratory burst,

https://doi.org/10.4168/aair.2023.15.2.246

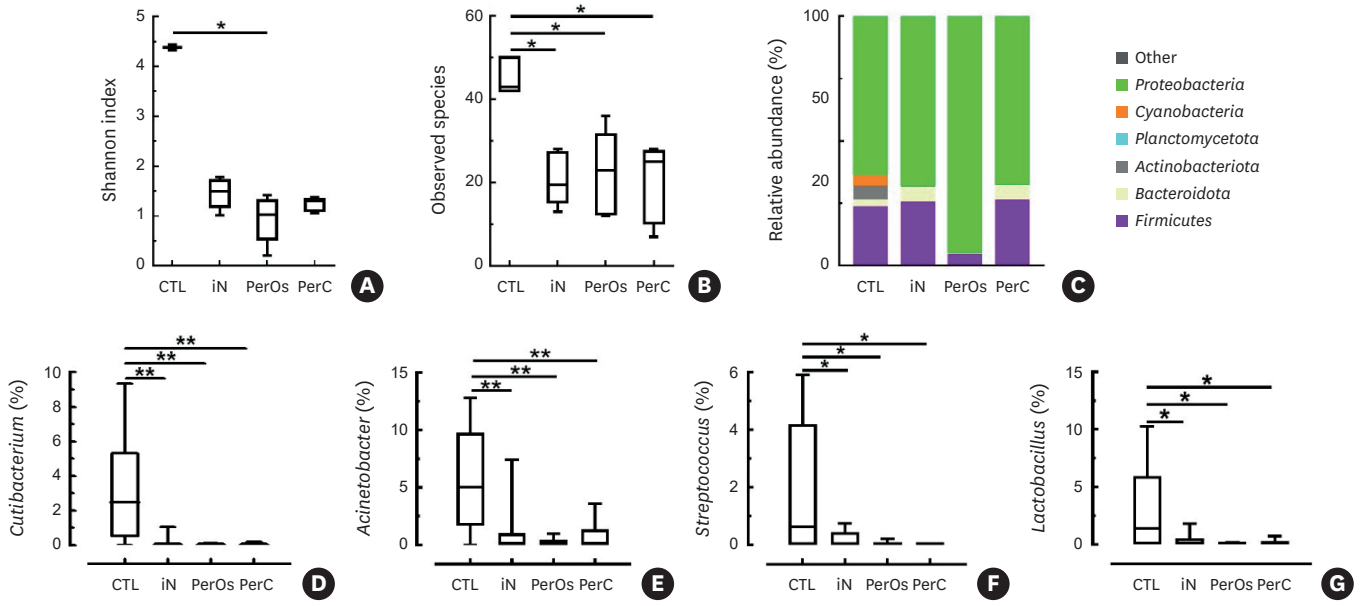

Fig. 5. The sensitization route is associated with a difference in lung microbiota composition. (A) The species diversity of the community was analyzed through Shannon's diversity index and (B) observed ASVs. (C) Pulmonary microbial phyla are represented at different taxonomic levels by showing changes in the relative abundance of *Cyanobacteria*, *Proteobacteria*, *Actinobacteria*, *Firmicutes*, and *Bacteroidetes* as a function of the sensitization pathway compared to the CTL. A significant pulmonary microbial genus level is represented in relative abundance to total bacteria for (D) *Cutibacterium*, (E) *Acinetobacteria*, (F) *Streptococcus*, and (G) *Lactobacillus*. The gray triangle indicates the CTL, the white circle indicates the iN, the white triangle indicates the PerOs, and the white square indicates the PerC. Data are represented by boxes with the mean, maximum and minimum and by the mean ± standard error of mean (n = 6).
CTL, control; iN, nasal route; PerOS, oral route; PerC, percutaneous route.
*P < 0.05, **P < 0.01.

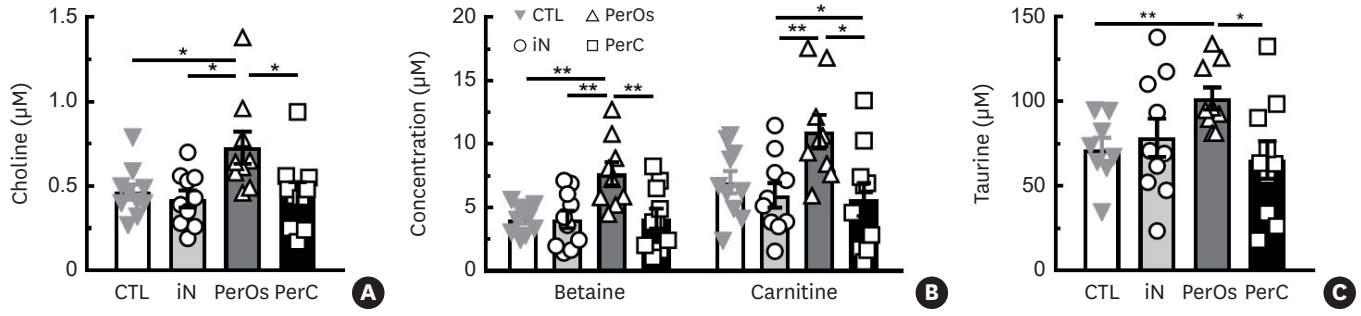

Fig. 6. The sensitization route is associated with differences in lung microbiota metabolites. Lung microbiota metabolite concentrations of (A) choline, (B) betaine, (C) carnitine and taurine were quantified by mass spectrometry. The gray triangle indicates the CTL, the white circle indicates the iN, the white triangle indicates the PerOs, and the white square indicates the PerC. Data are represented by the mean ± standard error of mean (n = 8).
CTL, control; iN, nasal route; PerOS, oral route; PerC, percutaneous route.
*P < 0.05, **P < 0.01.

was also increased in the PerOS mice compared to the other mice (**Fig. 6C**). Collectively, oral sensitization was correlated with a higher level of anti-inflammatory metabolites in the lung.

DISCUSSION

Asthma is a complicated disease characterized by an important phenotypic diversity, depending on respiratory function impairment severity, airway epithelial dysfunction, immune responses or endotypes, and microbiota dysbiosis. Skin, lung and intestinal epithelia are not only physical barriers but also powerful inducers of immune responses against

https://doi.org/10.4168/aair.2023.15.2.246

environmental agents. Sensitization pathways have been hypothesized to be the origin of phenotypic diversity in allergic diseases, especially in asthma. In this study, we established mouse models of allergic asthma with different sensitization routes and compared their phenotypes. Our results showed that typical asthmatic features, including eosinophilic infiltration, AHR, mucus production and high IgE levels, could be reproduced by different HDM sensitization route in mice. Interestingly, there were notable differences among them, including the region and severity of lung inflammation and epithelium integrity. These findings indicated that the pathophysiological pattern of asthma varies according to the mode of induction. These observations are in line with those of previous studies suggesting that HDM in the gut may potentiate sensitization[27] or HDM in the skin potentiate a Th17 response.[28] This airway inflammation can occur in the proximal to distal airways and lung parenchyma, resulting in lung hyperinflation due to extensive mucus plugging.[29]

In patients with asthma, the barrier function of the epithelium plays an important, but misunderstood role by disrupting tight junctions in the central and small airways and lung parenchyma.[30] Here, we demonstrated the influence of the route of sensitization on tight junction disruption. The mice sensitized via the cutaneous or respiratory route displayed an alteration in tight junction expression, while the orally sensitized mice did not. Similarly, a recent study modeled different inflammatory phenotypes in mice through the nasal or intraperitoneal routes.[31] Our results highlighted barrier dysfunction at the macroscopic level rather than a specific pathway within the epithelial barrier. Thus, our results should be confirmed by further studies at the protein level.

The sensitization route plays a critical role in the histological features of asthma, with cutaneous and intranasal exposure of the allergen inducing different disruptions of the epithelial barrier. Mucus overproduction is a characteristic consequence of epithelial barrier impairment in asthma. It has been shown that IL-17A increases mucin expression in human primary airway epithelial cells, indicating the association of mucus overexpression and Th17 inflammation.[31] Other studies in humans and mice supported these results.[32] *In vivo* studies have shown that allergen exposure promotes inflammation through the interaction of various immune cells, such as eosinophils, neutrophils, activated T lymphocytes, macrophages and dendritic cells. In particular, Th2 cytokines, including IL-4, IL-5, and IL-13, play critical roles in the development and maintenance of asthma. Here, airway inflammation was slightly enhanced by oral sensitization characterized by an increase in only eosinophils and specific IgE.

Th17 cells, involved in the pathogenesis of allergic asthma, was largely increased in the cutaneous- or nasal-sensitized mice.[33] In parallelTh2-dependent airway reactivity is enhanced in a more pronounced manner via the intranasal or cutaneous route, suggesting that the mode of sensitization can differentially alter the physical features of the airways. Our results suggested that animal models of asthma with different histopathological patterns and immune phenotypes can be established by varying the sensitization route (**Fig. 7**).

As a chronic inflammatory disease, asthma shows complex heterogeneity with various clinical phenotypes, depending on the interplay between environmental factors and various susceptibility genes. Many recent studies have begun to reveal the role of the microbiota in asthma pathogenesis, enhancing the understanding of this heterogeneous disorder.[34] Our current study explored the link between the route of sensitization and dysbiosis in a mouse model. In previous studies on the respiratory microbiome, many differences were reported between patients with asthma and healthy people, and among patients with different

https://doi.org/10.4168/aair.2023.15.2.246

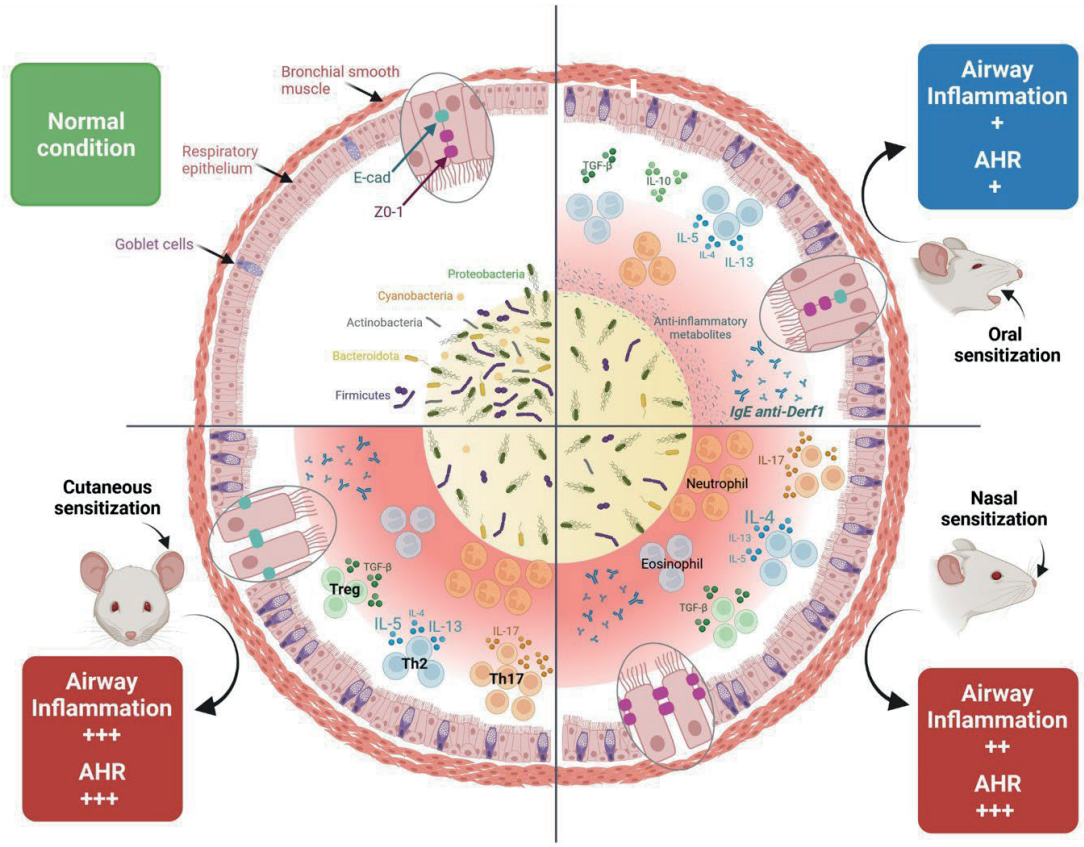

Fig. 7. The sensitization route influence in allergic asthma physiopathology. After sensitization and challenge with house dust mites, mice displayed an inflammatory response, epithelial barrier dysfunction and dysbiosis. However, oral sensitization induced a mild inflammatory response, epithelial barrier disruption, an increase in the Proteobacteria/Firmicutes ratio and anti-inflammatory metabolites. In contrast, nasal or percutaneous sensitization results in a severe inflammatory response and epithelial barrier damage associated with dysbiosis marked by an increase in *Bacteroidetes* abundance. These modulations affect asthma phenotypes/endotypes and demonstrate the role of sensitization in allergic asthma development.
AHR, airway hyperresponsiveness; E-cad, E-cadherin; ZO-1, zonula occludens-1; TGF, transforming growth factor; IL, interleukin; IgE, immunoglobulin E; Treg, regulatory T cell; Th, T helper cell.

clinical types of asthma.[35] We first observed a decrease in lung microbiota diversity and ASV regardless of the route of exposure. Since the quantitative lung microbiota was similar among the routes of exposure, we analyzed the respiratory microbiota composition at the phylum level. Among the upper respiratory tract microbiota, *Cyanobacteria* and *Actinobacteria* were more abundant in the naive mice than in the sensitized mice. On the contrary, the abundances of *Bacteroidetes* and *Firmicutes* were largely decreased in the mice sensitized via the oral route. At the genus level, *Cutibacterium*, linked to the skin condition of acne, was found to be significantly decreased in asthmatic mice. Other genera, such as *Acinetobacter*, *Lactobacillus*, and *Streptococcus,* were also found to have decreased abundance. *Acinetobacter* was known to be probiotics, and intranasal exposure suppressed asthma development through the inhibition of type 2 responses by modulating lung macrophage activation, shifting M2a and M2c macrophages to M2b macrophages.[36] Moreover, neonatal mice were protected from AHR when inhaled *Acinetobacter* was administered concurrently with HDM. *Acinetobacter* blocked the expansion of pulmonary IL-13+CD4+ T cells, whereas IL-13+ ILCs and IL-33 levels remained elevated.[37] Similarly, *Lactobacillus* decreased the number of granulocytes, the levels of Th2 and Th17 inflammatory cytokines in the lungs, and the airway inflammation score, and promoted the secretion of IL-10.[38] Interestingly, *Streptococcus* abundance was found to be decreased in children with severe wheezing compared to children with non-severe wheezing.[39] Moreover,

https://doi.org/10.4168/aair.2023.15.2.246

a decrease in the ratio of the *Streptococcus* genus to the other genera was found in individuals with atopic dermatitis compared to healthy controls.[40] We also observed an increase in proteobacteria in oral-sensitized mice which may be linked to an increase in *Haemophilus* that in turn may influence phenotype.[41] These results indicated that the predominant microbiota of the respiratory tract were different according to the route of sensitization in asthma. The dysbiosis linked to sensitizing pathway is likely correlated with different inflammation. However, at the genus level, similar differences were observed, suggesting dysfunction in the functional microbiota. Finally, in addition to quantitative and qualitative differences in lung microbiota affecting asthma characteristics, growing evidences suggest that functional properties remain a crucial point in the relationships between microbiota in healthy and disease states.[42] Here, oral sensitization is correlated with a higher level of anti-inflammatory metabolites in the lung as suggested by the link between choline and betaine with lower inflammatory marker as well as taurine and antioxidant effect.[43]

Our preliminary results demonstrated the large influence of route of exposure on subsequent allergic immune reaction, and could be useful for allergic prevention and mitigation especially in allergic progression. In fact, infant allergies, such as dermatitis and food allergy, often evolve toward allergic asthma in adulthood during the atopic march and route of sensitization influences immune cell recruitment at various mucosal sites a model of food allergy.[44] Thus, there is a connection between the different route of exposure and the subsequent immune response in allergies. These differences may have impact on disease severity and/or development, thus participating in the atopic march. However, our study is limited to a mouse model and should be extended to non-human primates and/or human cells to confirm our data. To finish with, we did not explore the impact of doses and nature of allergens, which should be taken into consideration and modify especially interactions between epithelial barriers and allergens. Despite these limitations, our study highlights the potential impact of exposure route on asthma phenotype.

ACKNOWLEDGMENTS

The author would like to thank the Cytocell platform for assistance with the flow cytometry analysis, and we would like to thank the Therassay platform for the use of respiratory equipment (Flexivent system, Plethysmography). We are grateful to the members of the UTE IRS-UN animal facility for the support they provided with the mice. We would also like to thank the MicroPicell platform for performing the histological preparation. We would like to thank Stallergenes Greer for kindly providing the HDM total extract. The authors thank the cluster LUNG innOvatiOn (LUNG O2) for logistic support. We thank M. DeCarvalho, A. Moui and C. Lebot for their experimental help. The authors thank the Genavie Foundation for funding support. The authors thank the Mibiogate consortium for their funding, material and engineering support. The authors thank L. Boussamet for collaborating on in silico microbiota metabolite analysis. The authors thank M. Croyal and S. Crossouard from the mass spectrometry platform of SFR-sante F. Bonamy for their collaboration.
This work was supported by a grant from the Mibiogate consortium and the Fondation du souffle, INRAe Transfert and the “Institut de Recherche en Santé Respiratoire des Pays de La Loire” IRSRPL. LUNG O2 is supported by the National Research Agency under the Programme d'Investissements d'Avenir (ANR-16-IDEX-0007), the Pays de la Loire Region research program and by the Institut de Recherche en Santé Respiratoire des Pays de la Loire”. The Genavie Foundation supported this project with a grant.

SUPPLEMENTARY MATERIAL

Supplementary Fig. S1

Lung sections were stained with HPS, PAS or transgelin (α-SMA) after paraffin inclusion and observed under a microscope. (A) Histological scores were calculated by measuring (B) bronchial epithelium thickness, (C) bronchial smooth muscle thickness, and (D) mucus-producing cells (n = 4–5).

Click here to view

REFERENCES

1. Bateman ED, Hurd SS, Barnes PJ, Bousquet J, Drazen JM, FitzGerald JM, et al. Global strategy for asthma management and prevention: GINA executive summary. Eur Respir J 2008;31:143-78.
PUBMED | CROSSREF
2. Bousquet J, Khaltaev N, Cruz AA, Denburg J, Fokkens WJ, Togias A, et al. Allergic Rhinitis and its Impact on Asthma (ARIA) 2008 update (in collaboration with the World Health Organization, GA(2)LEN and AllerGen). Allergy 2008;63 Suppl 86:8-160.
PUBMED | CROSSREF
3. Lourenço O, Fonseca AM, Taborda-Barata L. Demographic, laboratory and clinical characterisation of adult portuguese asthmatic patients. Allergol Immunopathol (Madr) 2007;35:177-83.
PUBMED | CROSSREF
4. Frøssing L, Silberbrandt A, Von Bülow A, Backer V, Porsbjerg C. The prevalence of subtypes of type 2 inflammation in an unselected population of patients with severe asthma. J Allergy Clin Immunol Pract 2021;9:1267-75.
PUBMED | CROSSREF
5. Galli SJ, Tsai M. IgE and mast cells in allergic disease. Nat Med 2012;18:693-704.
PUBMED | CROSSREF
6. Zosky GR, Sly PD. Animal models of asthma. Clin Exp Allergy 2007;37:973-88.
PUBMED | CROSSREF
7. Bates JH, Rincon M, Irvin CG. Animal models of asthma. Am J Physiol Lung Cell Mol Physiol 2009;297:L401-10.
PUBMED | CROSSREF
8. Haspeslagh E, Debeuf N, Hammad H, Lambrecht BN. Murine models of allergic asthma. Methods Mol Biol 2017;1559:121-36.
PUBMED | CROSSREF
9. Daubeuf F, Frossard N. Acute asthma models to ovalbumin in the mouse. Curr Protoc Mouse Biol 2013;3:31-7.
PUBMED | CROSSREF
10. Piggott DA, Eisenbarth SC, Xu L, Constant SL, Huleatt JW, Herrick CA, et al. MyD88-dependent induction of allergic Th2 responses to intranasal antigen. J Clin Invest 2005;115:459-67.
PUBMED | CROSSREF
11. Tsitoura DC, Blumenthal RL, Berry G, Dekruyff RH, Umetsu DT. Mechanisms preventing allergen-induced airways hyperreactivity: role of tolerance and immune deviation. J Allergy Clin Immunol 2000;106:239-46.
PUBMED | CROSSREF
12. Wilson RH, Whitehead GS, Nakano H, Free ME, Kolls JK, Cook DN. Allergic sensitization through the airway primes Th17-dependent neutrophilia and airway hyperresponsiveness. Am J Respir Crit Care Med 2009;180:720-30.
PUBMED | CROSSREF
13. Bourdin A, Adcock I, Berger P, Bonniaud P, Chanson P, Chenivesse C, et al. How can we minimise the use of regular oral corticosteroids in asthma? Eur Respir Rev 2020;29:190085.
PUBMED | CROSSREF
14. Lloyd CM, Hessel EM. Functions of T cells in asthma: more than just T_H2 cells. Nat Rev Immunol 2010;10:838-48.
PUBMED | CROSSREF

15. Akbari O, Freeman GJ, Meyer EH, Greenfield EA, Chang TT, Sharpe AH, et al. Antigen-specific regulatory T cells develop via the ICOS-ICOS-ligand pathway and inhibit allergen-induced airway hyperreactivity. Nat Med 2002;8:1024-32.
PUBMED | CROSSREF

16. Akbari O, DeKruyff RH, Umetsu DT. Pulmonary dendritic cells producing IL-10 mediate tolerance induced by respiratory exposure to antigen. Nat Immunol 2001;2:725-31.
PUBMED | CROSSREF

17. Campbell JD, Buckland KF, McMillan SJ, Kearley J, Oldfield WL, Stern LJ, et al. Peptide immunotherapy in allergic asthma generates IL-10-dependent immunological tolerance associated with linked epitope suppression. J Exp Med 2009;206:1535-47.
PUBMED | CROSSREF

18. Lewkowich IP, Herman NS, Schleifer KW, Dance MP, Chen BL, Dienger KM, et al. CD4+CD25+ T cells protect against experimentally induced asthma and alter pulmonary dendritic cell phenotype and function. J Exp Med 2005;202:1549-61.
PUBMED | CROSSREF

19. Strickland DH, Stumbles PA, Zosky GR, Subrata LS, Thomas JA, Turner DJ, et al. Reversal of airway hyperresponsiveness by induction of airway mucosal CD4+CD25+ regulatory T cells. J Exp Med 2006;203:2649-60.
PUBMED | CROSSREF

20. Huang YJ. The respiratory microbiome and innate immunity in asthma. Curr Opin Pulm Med 2015;21:27-32.
PUBMED | CROSSREF

21. Klein M, Colas L, Cheminant MA, Brosseau C, Sauzeau V, Magnan A, et al. Der p 2.1 peptide abrogates house dust mites-induced asthma features in mice and humanized mice by inhibiting DC-mediated T cell polarization. Front Immunol 2020;11:565431.
PUBMED | CROSSREF

22. Baqueiro T, Russo M, Silva VM, Meirelles T, Oliveira PR, Gomes E, et al. Respiratory allergy to *Blomia tropicalis*: immune response in four syngeneic mouse strains and assessment of a low allergen-dose, short-term experimental model. Respir Res 2010;11:51.
PUBMED | CROSSREF

23. Johnson JR, Wiley RE, Fattouh R, Swirski FK, Gajewska BU, Coyle AJ, et al. Continuous exposure to house dust mite elicits chronic airway inflammation and structural remodeling. Am J Respir Crit Care Med 2004;169:378-85.
PUBMED | CROSSREF

24. Wavrin S, Bernard H, Wal JM, Adel-Patient K. Cutaneous or respiratory exposures to peanut allergens in mice and their impacts on subsequent oral exposure. Int Arch Allergy Immunol 2014;164:189-99.
PUBMED | CROSSREF

25. Wavrin S, Bernard H, Wal JM, Adel-Patient K. Influence of the route of exposure and the matrix on the sensitisation potency of a major cows' milk allergen. Clin Transl Allergy 2015;5:3.
PUBMED | CROSSREF

26. Bihouée T, Bouchaud G, Chesné J, Lair D, Rolland-Debord C, Braza F, et al. Food allergy enhances allergic asthma in mice. Respir Res 2014;15:142.
PUBMED | CROSSREF

27. Tulic MK, Vivinus-Nébot M, Rekima A, Rabelo Medeiros S, Bonnart C, Shi H, et al. Presence of commensal house dust mite allergen in human gastrointestinal tract: a potential contributor to intestinal barrier dysfunction. Gut 2016;65:757-66.
PUBMED | CROSSREF

28. Chesné J, Braza F, Chadeuf G, Mahay G, Cheminant MA, Loy J, et al. Prime role of IL-17A in neutrophilia and airway smooth muscle contraction in a house dust mite-induced allergic asthma model. J Allergy Clin Immunol 2015;135:1643-1643.e3.
PUBMED | CROSSREF

29. Hamid Q. Pathogenesis of small airways in asthma. Respiration 2012;84:4-11.
PUBMED | CROSSREF

30. Loxham M, Davies DE, Blume C. Epithelial function and dysfunction in asthma. Clin Exp Allergy 2014;44:1299-313.
PUBMED | CROSSREF

31. Tan HT, Hagner S, Ruchti F, Radzikowska U, Tan G, Altunbulakli C, et al. Tight junction, mucin, and inflammasome-related molecules are differentially expressed in eosinophilic, mixed, and neutrophilic experimental asthma in mice. Allergy 2019;74:294-307.
PUBMED | CROSSREF

32. Xia W, Bai J, Wu X, Wei Y, Feng S, Li L, et al. Interleukin-17A promotes MUC5AC expression and goblet cell hyperplasia in nasal polyps via the Act1-mediated pathway. PLoS One 2014;9:e98915.
PUBMED | CROSSREF

33. Ramakrishnan RK, Al Heialy S, Hamid Q. Role of IL-17 in asthma pathogenesis and its implications for the clinic. Expert Rev Respir Med 2019;13:1057-68.
PUBMED | CROSSREF

34. Herbst T, Sichelstiel A, Schär C, Yadava K, Bürki K, Cahenzli J, et al. Dysregulation of allergic airway inflammation in the absence of microbial colonization. Am J Respir Crit Care Med 2011;184:198-205.
PUBMED | CROSSREF

35. Fazlollahi M, Lee TD, Andrade J, Oguntuyo K, Chun Y, Grishina G, et al. The nasal microbiome in asthma. J Allergy Clin Immunol 2018;142:834-843.e2.
PUBMED | CROSSREF

36. Kang H, Bang JY, Mo Y, Shin JW, Bae B, Cho SH, et al. Effect of *Acinetobacter lwoffii* on the modulation of macrophage activation and asthmatic inflammation. Clin Exp Allergy 2022;52:518-29.
PUBMED | CROSSREF

37. Saglani S, Gregory LG, Manghera AK, Branchett WJ, Uwadiae F, Entwistle LJ, et al. Inception of early-life allergen-induced airway hyperresponsiveness is reliant on IL-13+CD4+ T cells. Sci Immunol 2018;3:eaan4128.
PUBMED | CROSSREF

38. Li L, Fang Z, Lee YK, Zhao J, Zhang H, Lu W, et al. Prophylactic effects of oral administration of *Lactobacillus casei* on house dust mite-induced asthma in mice. Food Funct 2020;11:9272-84.
PUBMED | CROSSREF

39. Robinson PF, Fontanella S, Ananth S, Martin Alonso A, Cook J, Kaya-de Vries D, et al. Recurrent severe preschool wheeze: from prespecified diagnostic labels to underlying endotypes. Am J Respir Crit Care Med 2021;204:523-35.
PUBMED | CROSSREF

40. Yu L, Deng YH, Huang YH, Ke HJ, Guo Y, Wu JL. Comparison of gut microbiota between infants with atopic dermatitis and healthy controls in Guangzhou, China. J Asthma Allergy 2021;14:493-500.
PUBMED | CROSSREF

41. Chung KF. Potential role of the lung microbiome in shaping asthma phenotypes. Ann Am Thorac Soc 2017;14:S326-31.
PUBMED | CROSSREF

42. de Vos WM, Tilg H, Van Hul M, Cani PD. Gut microbiome and health: mechanistic insights. Gut 2022;71:1020-32.
PUBMED | CROSSREF

43. Kulczyński B, Sidor A, Gramza-Michałowska A. Characteristics of selected antioxidative and bioactive compounds in meat and animal origin products. Antioxidants 2019;8:335.
PUBMED | CROSSREF

44. Briard M, Guinot M, Grauso M, Guillon B, Hazebrouck S, Bernard H, et al. Route of sensitization to peanut influences immune cell recruitment at various mucosal sites in mouse: an integrative analysis. Nutrients 2022;14:790.
PUBMED | CROSSREF